

# Determination of ultrahigh molar mass of polyelectrolytes by Taylor dispersion analysis

Xiaoling Leclercq<sup>1</sup>, Laurent Leclercq<sup>1</sup>, Alexis Guillard<sup>2</sup>, Laurent Rodriguez<sup>2</sup>, Olivier Braun<sup>2</sup>, Cédric Favero<sup>2</sup> and Hervé Cottet<sup>1,\*</sup>

<sup>1</sup> IBMM, University of Montpellier, CNRS, ENSCM, Montpellier, France

<sup>2</sup> SNF Floerger, Andrézieux, France

## ABSTRACT

Taylor dispersion analysis (TDA) was successfully applied to obtain broadly distributed, ultrahigh molar masses of industrial anionic polyacrylamides (IPAMs) up to  $25 \times 10^6$  g/mol, far beyond the detection limit of SEC (about  $7.3 \times 10^6$  g/mol for anionic polyacrylamides standards). Two protocols of TDA differing in capillary surface and rinsing procedure were employed: (i) bare fused silica capillaries under intensive between-run rinsing with 1M NaOH, and (ii) capillaries coated with polyelectrolyte multilayers composed of polydiallyldimethylammonium chloride polycation and sodium polystyrenesulfonate polyanion under simple rinsing with background electrolyte. Both cases led to similar results and in agreement with those obtained by static light scattering, the rinsing capillary step being much shorter in the second case (8 min instead of 30 min). The data processing of the obtained taylorgrams was realized using multiple-Gaussian fitting of the overall taylorgrams, by separating the contribution of low molar mass impurities from the polymeric profiles, and by determining the mean hydrodynamic radii and diffusion coefficients of the polymers. The molar masses of ultra-high molar mass industrial anionic polyacrylamides were derived from the hydrodynamic radii according to  $\log R_h$  versus  $\log M_w$  linear correlation established with APAM standards. Compared to capillary gel electrophoresis for which the size separation was only feasible up to  $M_w \sim 10 \times 10^6$  g/mol due to field induced polymer aggregation, TDA largely extended the range of accessible molar mass with easy-to-run and time saving assays.

**Keywords:** Taylor dispersion analysis, size-based separations, ultrahigh molar mass determination, polyacrylamides

\* CORRESPONDING AUTHOR

Tel: +33 4 6714 3427, Fax: +33 4 6763 1046. E-mail: herve.cottet@umontpellier.fr

34

35

36

37 **Highlights**

38

39 • Linear  $\log R_h$  vs  $\log M_w$  correlation obtained by TDA on a broad range of molar masses

40 • Analysis of ultrahigh molar mass polyacrylamides up to  $25 \times 10^6$  g/mol by TDA

41 • TDA results were consistent with those obtained by static light scattering

42 • TDA offers a straightforward, absolute, easy-to-run and rapid method for size-based  
43 characterization

## 44 1. Introduction

45

46 In numerous industrial applications such as wastewater treatment and enhanced oil  
47 recovery, high to ultrahigh molar mass (above  $1 \times 10^6$  g/mol) anionic poly(acrylic acid-co-  
48 acrylamide)s have been playing an important role as media thickener for decades [1-3].  
49 However, characterization of unusually high molar mass polyelectrolytes remains challenging  
50 and laborious. Due to inherent separation limits of conventional SEC, such as abnormal  
51 elution due to polymer adsorption or chain breakage in the column packing, polyacrylamide  
52 copolymers with molar masses higher than  $7.5 \times 10^6$  g/mol cannot be analyzed by SEC [4-7].  
53 It was found that higher molar mass polyelectrolytes, when passing through a porous medium,  
54 are sensible to mechanical degradation based on coil-stretch transition of polymer chains  
55 above a critical extension rate, leading to central scissions of polymers in diluted regime and  
56 random scissions in semi-diluted regime [5]. Moreover, largely polydisperse polymers usually  
57 elute in abnormal overlapped peaks that cannot be resolved by SEC. Other techniques are  
58 pursued with certain success including in-batch multi-angle laser light scattering (MALLS)  
59 [9, 10] and asymmetric field-flow fractionation [11, 12]. In a previous study [13], we reported  
60 the performance of capillary gel electrophoresis (CGE) with 2-hydroxyethyl cellulose (HEC)  
61 as sieving polymer for the characterization of ultrahigh molar mass industrial polyacrylamides  
62 (IPAMs) up to  $10 \times 10^6$  g/mol, in agreement with the results obtained by static light scattering  
63 (SLS). However, the limit of CGE lied in the problem of aggregation of the IPAMs under  
64 action of electric fields [14], as well as field-dependent biased reptation of the polyelectrolyte  
65 chains.

66 To alleviate the problem of aggregation, Taylor dispersion analysis (TDA) is an interesting  
67 alternative that applies a mobilizing pressure instead of an electric field as driving force in the  
68 capillary. TDA is based on the dispersion of sample plug injected in narrow capillary  
69 (typically 50  $\mu$ M i.d.) under a Poiseuille-like flow. The Taylor dispersion is due to the  
70 combination of the convective parabolic velocity profile with molecular diffusion. TDA is an  
71 absolute method (no calibration is required) allowing to determine the determine diffusion  
72 coefficients ( $D$ ) from the dispersion (temporal variance) of the elution profile.  $D$  and  
73 hydrodynamic radii ( $R_h$ ) of large varieties of solutes were determined by TDA including  
74 macromolecules [15-18], nanoparticles [19-21], proteins [22, 23] and more recently, vaccine  
75 antigens and/or adjuvants [24]. Regarding the limits of analysis of TDA, it is predicted that  $R_h$   
76 should be smaller than 210 nm on a 50  $\mu$ m i.d. capillary to keep the relative error  $\varepsilon$  of  
77 diffusion coefficient  $D$  below 5%. For higher solute sizes, convective and hydrodynamic

78 chromatography (HDC) regimes would occur, leading to non-Gaussian elution profiles (see  
79 e.g. Fig. S11 to visualize the different regimes) [22].

80 In this work, we investigated the potential of TDA for the size (hydrodynamic radius) and  
81 molar mass characterization of high to ultrahigh molar mass industrial anionic poly(acrylic  
82 acid-co-acrylamide)s (IPAMs). Due to the concern of maintaining the ultrahigh molar mass  
83 IPAMs within Taylor regime, the increase of the background electrolyte ionic strength has  
84 been investigated to get more compact polymer conformations. To check the impact of the  
85 capillary wall surface on the TDA results, two experimental protocols using (i) bare  
86 capillaries combined with rigorous between-run rinsing with 1M NaOH and (ii) SMIL  
87 (Successive Multiple Ionic Layers)-coated capillaries based on  
88 polydiallyldimethylammonium chloride as a polycation and sodium polystyrene sulfonate as a  
89 polyanion with simple rinsing with background electrolyte.

90

91

## 92 **2. Experimental**

93

### 94 *2.1. Chemicals*

95 Tris(hydroxymethyl)aminomethane (TRIS) and polydiallyldimethylammonium chloride  
96 (PDADMAC) 20%,  $M_w = 400,000-500,000$  g/mol, 4-(2-Hydroxyethyl)piperazine-1-ethane  
97 sulfonic acid (HEPES), tris(hydroxyméthyl) aminométhane (Tris), sodium hydroxide, lithium  
98 chloride anhydrous, and lithium hydroxide were purchased from Sigma-Aldrich (Saint  
99 Quentin Fallavier, France), sodium polystyrenesulfonate (PSS),  $M_w=70,000$  g/mol, from  
100 Acros (Illkirch, France), hydrochloric acid and potassium chloride from VWR (Fontenay-  
101 sous-Bois, France), and finally sodium chloride from Fluka (Illkirch, France).

102

### 103 *2.2. Samples*

104 The anionic poly(acrylic acid-co-acrylamide)s industrial samples (IPAMs) and standard  
105 samples (APAMs) were provided by SNF Floerger (Andrézieux, France). APAMs were  
106 synthesized from monomers of sodium acrylate and acrylamide by controlled radical  
107 polymerization (CRP) with narrowly distributed molar mass and anionicity [26]. IPAMs were  
108 obtained by hydrolysis of polyacrylamide in a NaOH medium to the defined anionicity. The  
109 molar mass and polydispersity index (PDI) of the APAMs were determined by SEC-MALS  
110 [7], and the molar mass of the IPAMs by batch-SLS (see Table 1).

111 Stock solutions of APAMs and IPAMs were prepared in small scale by dissolving 50 mg  
112 sample in 10 mL background electrolyte (BGE) under magnetic stirring at 500 rpm for 6 h.  
113 The BGE was composed of 20 mM Tris/HCl buffer at pH 8.0 containing 35.5 mM LiCl (total  
114 ionic strength  $I = 46.5$  mM). For the study of the impact of ionic strength, BGE of the same  
115 Tris/Cl buffer containing 1M NaCl or 1M KCl were used. The stock solutions were kept at  
116 5°C before and after use. The test solutions were then prepared by dilution of the stock  
117 solutions with BGE to the injected concentration of 2 g/L and homogenized using an orbital  
118 mixer for 3 min. All samples were used non-filtered.

119

### 120 *2.3. Size-Exclusion Chromatography (SEC-MALS)*

121 Weight and number average molar mass, PDI, and radius of gyration of APAMs were  
122 obtained by a SEC-MALS Agilent 1260 Infinity I system (Agilent Technologies, Les Ulis,  
123 France). It consisted of an on-line degasser, a high-pressure pump, an automatic sampler, a 8  
124 × 300 mm SEC column packed with polyhydroxymethacrylate-based gel (OHpak Shodex  
125 columns, Showa Denko, Munich, Germany), a multi-angle light scattering (MALS) detector  
126 (Dawn Heleos II, Wyatt Technology, Toulouse, France) and a refractive index (RI) detector  
127 (Optilab, Wyatt Technology, Toulouse, France). Experimental conditions were given in [7].  
128 Buffer containing 0.5 M sodium nitrate and 55 mM HEPES (pH 8) was used as the eluent that  
129 was filtered through a 0.1 μm cellulose membrane before use. The flow rate was set at 0.3  
130 mL/min. Samples of 0.02% (w/V) concentration in the eluent were filtered through a 1.2 μm  
131 cellulose membrane before injection. The injection volume was 100 μL. The detectors of  
132 MALS and RI were kept at room temperature. The refractive index increment ( $dn/dc$ ) of the  
133 samples were measured by using the Optilab detector. Data acquisition and processing were  
134 achieved by the ASTRA software (version 6.1, Wyatt Technologies).

135

### 136 *2.4. SLS*

137 SLS batch analysis was carried out on the Dawn Heleos II equipment (see 2.3). Polymer  
138 solutions were prepared in 0.5 M sodium nitrate at 0.5 wt % and mixed under mechanical  
139 stirring (at 400 rpm) at room temperature for 2 h till dissolution. The 0.5 wt % polymer  
140 solutions were further diluted to 0.01 wt % under stirring with a magnetic stirrer at 200 rpm  
141 for 1 h, then filtered through 1.2 μm syringe filters to remove dusts and other large particle  
142 contaminants. The filtered solutions were diluted sequentially to 4-5 different concentrations  
143 by two syringe pumps before injection into the MALS detector. The MALS cell temperature

144 was set at 30°C, the flow rate at 0.3 mL/min. The scattering data were collected at 17 different  
145 angles with an incident laser wavelength of 664 nm. Calibration of the MALS detector was  
146 performed using HPLC grade toluene. The data analysis was conducted using the Astra 6.1  
147 software (see 2.3). In a batch MALS measurement, the angular and concentration dependent  
148 light scattering data were fitted with Ornstein-Zernick equation:

$$149 \quad \frac{R}{KC} = M_w \left( 1 + \frac{2q^2 R_g^2}{3D_f} \right)^{\frac{D_f}{2}} \quad (1)$$

150 where  $R$  is the excess Rayleigh ratio,  $K$  is the optical constant,  $C$  is the polymer concentration,  
151  $M_w$  is the weight-average molar mass,  $D_f$  is the fractional size,  $q$  is the scattering factor and  $R_g$   
152 is the radius of gyration.

153

#### 154 2.5. Taylor dispersion analysis (TDA)

155 TDA experiments were performed on a Beckman P/ACE MDQ apparatus (AB Sciex Life  
156 Sciences Holding, Villebon-sur-Yvette, France). Capillaries were prepared from a fused silica  
157 tubing (Photonlines, St Grégoire, France) with dimensions of 60 cm (50 cm to the detector) ×  
158 50 μm ID. Capillaries were first activated by successive flushing at 20 psi with 1 M NaOH for  
159 30 min, 0.1 M NaOH for 10 min, Milli-Q water for 10 min, and finally background electrolyte  
160 (BGE) for 10 min. BGE was 20 mM Tris/HCl with 35.5 mM LiCl,  $I = 46.5$  mM, pH 8.0. For  
161 the study of the impact of ionic strength on hydrodynamic radii, BGE was also prepared by  
162 adding 1M NaCl or 1M KCl instead of 35.5 mM LiCl.

163 Protocol of intensive between-run rinsing consisted of successively flushing the bare  
164 capillary with 1 M NaOH at 35 psi for 10 min, 0.1 M NaOH at 20 psi for 5 min, Milli-Q water  
165 at 20 psi for 5 min and BGE at 20 psi for 10 min, leading to total rinsing time of 30 min.

166 In a second approach, capillaries were coated as following: (i) activation with 1 M NaOH  
167 for 20 min at 20 psi, (ii) flushing with a solution of PDADMAC polycation at 3 g/L in 20 mM  
168 HEPES pH 7.4 at 20 psi for 7 min, (iii) rinsing with 20 mM HEPES pH 7.4 at 20 psi for 3  
169 min, (iv) flushing with a solution of PSS polyanion at 3 g/L in 20 mM HEPES pH 7.4 at 20  
170 psi for 7 min, (v) rinsing with 20 mM HEPES pH 7.4 at 20 psi for 3 min, and (vi) repetition of  
171 the (ii) to (v) steps. (PDADMAC/PSS)<sub>2</sub> SMIL coated capillary was finally rinsed with BGE  
172 for 8 min before sample injection. Between-run rinsing was carried out with BGE at 20 psi for  
173 8 min.

174 Samples were injected hydrodynamically at 0.5 psi for 7 s. The mobilizing pressure was  
 175 0.4 psi. UV absorption was detected at 200 nm. Temperature was set at 25°C.

176

## 177 2.6. Theoretical aspects

178 In TDA [27-29], when a solute plug is injected into a fluid flowing under laminar  
 179 Poiseuille profile through a capillary, it spreads out under the combined action of molecular  
 180 diffusion and the variation of velocity over the cross-section. The distribution of  
 181 concentration thus generated is centred on a point which moves with the mean speed of flow.  
 182 The elution profile is recorded at a certain distance from the injection point, via UV  
 183 absorbance of the polymer solute through the capillary tube. For a single size population, the  
 184 elution profile is normally distributed (Gaussian), as far as two conditions are satisfied: (i) the  
 185 axial diffusion should be negligible compared to convection (*i.e.* the Péclet number  $P_e =$   
 186  $R_c u/D > 40$ ) where  $R_c$  is the capillary radius,  $u$  is the linear velocity and  $D$  is the molecular  
 187 diffusion coefficient, and (ii) the average elution time  $t_0$  should be longer than the  
 188 characteristic diffusion time  $\tau$  of the solute (*i.e.*  $\tau = t_0 D/R_c^2 > 1.25$ ) [25].

189 For polydisperse samples, the taylorgram is a sum of Gaussians [17]:

$$190 \quad S(t) = \sum_{i=1}^n S_i(t) = \sum_{i=1}^n \frac{A_i}{\sigma_i \sqrt{2\pi}} \exp \left[ \frac{-(t-t_0)^2}{2\sigma_i^2} \right] \quad (2)$$

191 where  $S(t)$  is the elution signal at time  $t$ ,  $S_i(t)$  the Gaussian of the component  $i$  and  $\sigma_i$  is the  
 192 temporal variance of the component  $i$ . The temporal variance  $\sigma^2$  of the overall taylorgram is  
 193 calculated by integration of the taylorgram using Eq. 3:

$$194 \quad \sigma^2 = \frac{\int S(t)(t-t_0)^2 dt}{\int S(t) dt} \quad (3)$$

195 From the overall temporal variance, an average diffusion coefficient  $\langle D \rangle$  can be deduced  
 196 from Eq. 4:

$$197 \quad \langle D \rangle = \frac{R_c^2 t_0}{24 \sigma^2} = \frac{R_c^2 t_0}{24} \frac{\int_0^\infty S(t) dt}{\int_0^\infty S(t)(t-t_0)^2 dt} \quad (4)$$

198 Finally, the average hydrodynamic radius  $\langle R_h \rangle$  (a weight-average value for mass  
 199 concentration sensitive detector) is derived from Stokes-Einstein equation (Eq. 5):

$$200 \quad \langle R_h \rangle = \frac{k_B T}{6\pi\eta\langle D \rangle} \quad (5)$$

201 In this work, data processing of taylorgrams including Gaussian fitting (up to 3 Gaussians  
 202 using Excel solver), calculation temporal variances, diffusion coefficients and hydrodynamic  
 203 radii of the polymers were achieved with a lab-made Excel spreadsheet.

204

### 205 3. Results and discussion

206

207 The objective of this work was to develop and apply a TDA methodology to characterize  
208 the size (hydrodynamic radius) and molar mass of ultrahigh molar mass industrial samples  
209 (IPAM). All samples possess an anionicity between 27 and 33%. Since TDA gives access to  
210 the diffusion coefficient (and hydrodynamic radius) instead of molar masses,  $\log R_h$  vs  $\log M_w$   
211 correlation was experimentally determined by TDA using 6 standard samples (APAMs) of  
212 molar mass ranging between 2.2 kDa and 7.3 MDa. These APAM standards were fully  
213 characterized by SEC with relatively narrow PDI ranging between 1.1 and 1.5 (see Fig. SI2  
214 for the molar mass distributions). The molar masses of 5 IPAM samples were obtained by  
215 SLS and found between 6.5 MDa and 25 MDa (see Fig. SI3 for the molar mass determination  
216 by SLS). All APAM and IPAM predetermined characteristics are provided in Table 1.

217 Efforts to improve the robustness of TDA data was emphasized on minimizing the  
218 adsorption of anionic polyacrylamides onto the capillary surface that is governed by an  
219 equilibrium between attractive interactions (H-bonding between silanol groups present at the  
220 capillary wall surface and amide groups of the polymer) and electrostatic repulsion,  
221 depending on several parameters including pH, molar mass and dispersity of the polymer and  
222 ionic strength of BGE [31-33]. In this study, pH of the background electrolyte (BGE) was set  
223 at 8.0, at which the capillary surface was negatively charged and the anionic polyacrylamides  
224 remained stable without remarkable hydrolysis. To keep the capillary wall under 'steady-state  
225 conditions' to achieve good intra-capillary repeatability, two different protocols were  
226 employed for comparison. In the first case, an intensive between-run rinsing process using 1  
227 M NaOH at 35 mbar for 10 min followed by 0.1 M NaOH at 20 psi for 5 min, Milli-Q water  
228 at 20 psi for 5 min and BGE at 20 psi for 10 min, was undertaken in order to eliminate  
229 previous history of the fused silica capillary before a new run, especially when ultrahigh  
230 molar mass polymers were assayed, with the expense of re-equilibration time (for a total  
231 rinsing time of 30 min). In the second case, the capillary surface was coated with SMIL [34,  
232 35], namely two PADMAC/PSS bilayers, to enhance electrostatic repulsion between the  
233 capillary wall and the analytes, using simple between-run rinsing with BGE for 8 min only.  
234 The reproducibility of TDA in  $R_h$  determination was checked by intra-capillary repeatability  
235 by repeating 3 assays per sample on the same capillary and inter-capillary reproducibility by  
236 running all samples successively on 3 different capillaries.

237

#### 238 3.1. TDA on bare fused silica capillary

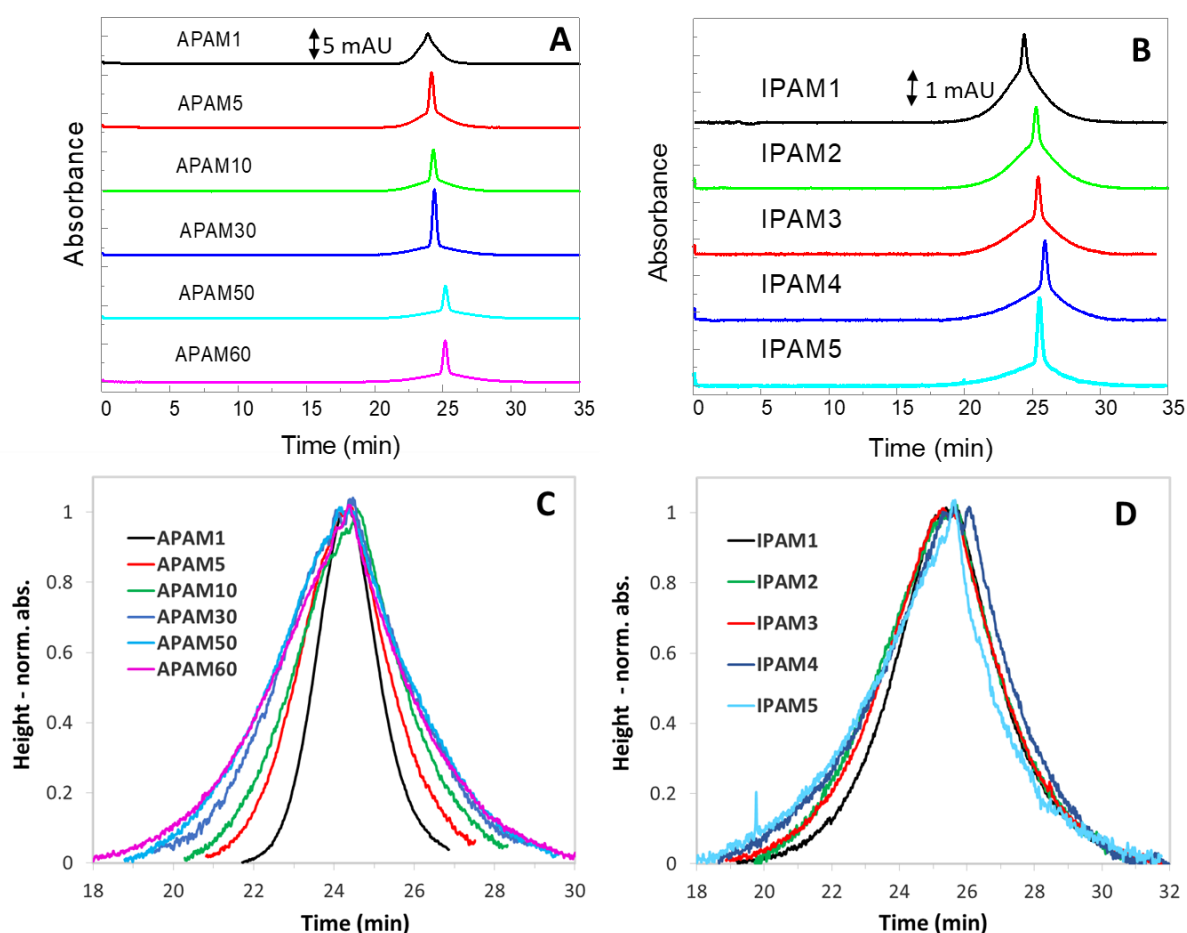


239 In TDA, the original taylorgrams (Fig. 1A for APAMs and Fig. 1B for IPAMs) were  
240 bimodal and contained an additional sharp peak that is due to the residual monomers and  
241 dimers as well as UV absorbing impurities such as urea, according to the provider. To extract  
242 hydrodynamic information of the polymer, each taylorgram was deconvoluted into 2 to 3  
243 Gaussian profiles using Excel Solver according to eq. (2). After subtraction of the small  
244 molecule contribution that corresponded to sizes between 0.38 nm and 0.60 nm, the remaining  
245 polymer profile was obtained and shown in Fig. 1C (for APAMs) and Fig. 1D (for IPAMs)  
246 with normalization at the maximum intensity for better interpretation. Narrowly distributed  
247 APAMs appeared relatively symmetric, and peak widths broadened systematically with  
248 increasing the molar mass, as expected according to Taylor dispersion. Slight distortion of the  
249 elution profile could be observed for the IPAM samples and was likely due to some polymer  
250 adsorption on the capillary wall that was not observed with APAMs. To avoid any bias in the  
251 average size determination, Gaussian fitting and calculation of the peak variance  $\sigma^2$  were only  
252 operated on the left half part of the taylorgram relative to the peak apex ( $t_0$ ).

253 All the hydrodynamic radius values obtained by TDA are presented in Table 1. To get a  
254 better insight about the repetability / reproducibility of the TDA measurements,  $n = 3$   
255 repetitions on  $m=3$  fused silica capillaries were performed. RSD on the average  $R_h$   
256 determination were always below 10% for both repeatability and reproducibility. Fig. 2 shows  
257 the  $\log R_h - \log M_w$  correlations lines obtained for the APAM standards (see plain blue dots  
258 and triangles for 20 mM Tris/HCl pH 8.0 with 35.5 mM LiCl eluent ( $I = 46.5$  mM)). Inter-  
259 capillary mean hydrodynamic radii are presented in this Figure with inter-capillary RSD as  
260 error bars. The molar masses used for this representation were obtained by SEC-MALS for  
261 APAM samples and by SLS for IPAM samples (see sections 2.3 and 2.4 for experimental  
262 conditions and see Table 1 for the data). The least squared regression displays good  
263 correlation ( $\langle R_h \rangle = 31.020 \times M_w^{0.5346}$ ,  $R^2 = 0.9926$ , with  $M_w$  in  $10^6$  g/mol and  $R_h$  in nm) and  
264 extended into the data range of IPAMs with very good agreement, on a range of  $R_h$  reaching  
265 up to 183.7 nm for IPAM5. This result proves that the experimental TDA conditions allows a  
266 true (non-biased) determination of large polymer sizes, even at moderate ionic strength (46.5  
267 mM). It is worth noting that the conditions of validity of the Taylor regime were always  
268 fulfilled (i.e.  $P_e = R_c u / D > 40$  and  $\tau = t_0 D / R_c^2 > 1.25$ ) for all polymer samples, even for the  
269 largest IPAM5 ( $P_e \sim 4400$ ;  $\tau \sim 4.5$ ). This was ensured by relatively low mobilization pressure  
270 to let the time to the large polymer solutes to average the parabolic velocity profile during the  
271 analysis time. Using the  $\log R_h - \log M_w$  correlation obtained with the APAM samples, it was

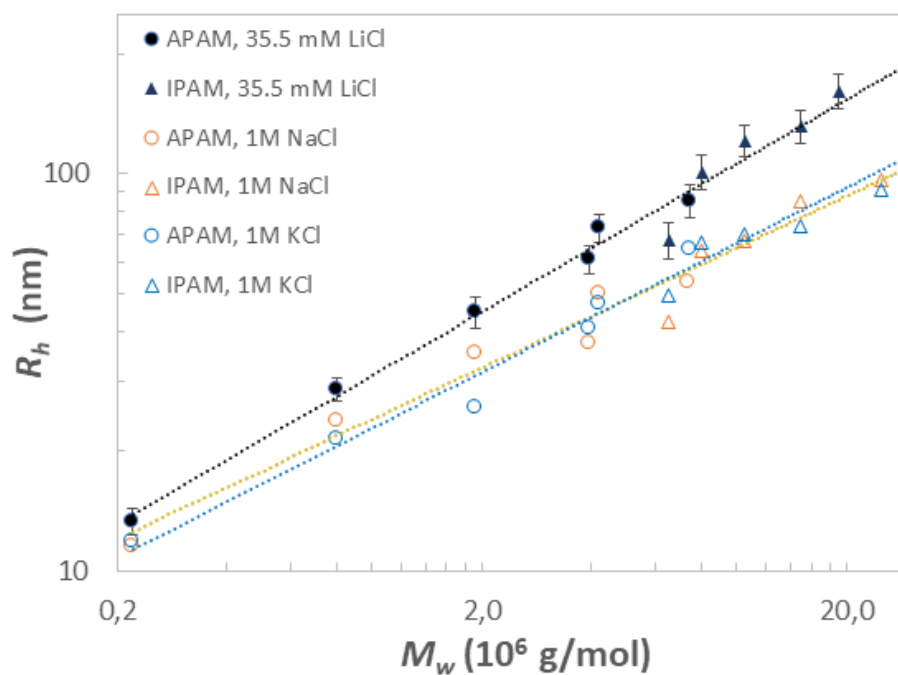
272 possible to determine the TDA molar masses ( $M_{wI, TDA}$ ) by using the reciprocal of the  $R_h - M_w$   
 273 correlation ( $M_w = 0.00162 \times \langle R_h \rangle^{1.8706}$ , for bare fused silica capillary (case 1) and  $M_w =$   
 274  $0.00195 \times \langle R_h \rangle^{1.7986}$ , for PDADMAC/PSS SMIL-coated capillary (case 2), with  $M_w$  in  $10^6$   
 275 g/mol and  $R_h$  in nm). Regarding the limit in size that can be determined by TDA due to  
 276 occurrence of the hydrodynamic chromatography regime that can affect the accuracy of the  $R_h$   
 277 determination, a maximum  $R_h$  value of 212 nm is expected as the upper limit in size if we  
 278 accept a maximum relative error of 5% (as calculated by  $R_h \leq 0.17 \times R_c \times \varepsilon$ , where  $\varepsilon$  is the  
 279 relative error [22]).

280



281

282 **Figure 1.** Original taylorgrams of poly(acrylic acid-co-acrylamide) standards (APAMs) (A) and industrial  
 283 samples (IPAMs) (B), and the corresponding height normalized taylorgrams subtracted from small molecules  
 284 contribution (C and D, respectively). Experimental conditions: fused silica capillary  $50 \mu\text{m ID} \times 60 \text{ cm}$  (50 cm to  
 285 the detector). Eluent: 20 mM Tris/HCl with 35.5 mM LiCl,  $I = 46.5 \text{ mM}$ , pH 8.0. Mobilization pressure: 0.4 psi.  
 286 Injection: 0.5 psi, 7 s. Injected sample concentration: 2 g/L in eluent. UV detection at 200 nm. Temperature:  
 287 25°C. Between-run rinsing: 1 M NaOH at 35 psi for 10 min, 0.1 M NaOH at 20 psi for 5 min, Milli-Q water at  
 288 20 psi for 5 min, and eluent at 20 psi for 10 min.



289

290 **Figure 2.**  $\log R_h - \log M_w$  correlations obtained for poly(acrylic acid-co-acrylamide)s standards (APAMs) and  
 291 industrial samples (IPAMs) using 20 mM Tris/HCl pH 8.0 eluents containing 35.5 mM LiCl, 1 M NaCl or 1 M  
 292 KCl. Least-squared regressions are, with  $M_w$  in  $10^6$  g/mol and  $R_h$  in nm:  $\langle R_h \rangle = 31.020 \times M_w^{0.5346}$ ,  $R^2 = 0.9926$  for  
 293 35.5 mM LiCl, error bar =  $\pm 1$  RSD ( $n = 3$ );  $R_h = 24.398 \times M_w^{0.4546}$ ,  $R^2 = 0.9609$  for 1 M NaCl and  $R_h =$   
 294  $18.328 \times M_w^{0.5109}$ ,  $R^2 = 0.9251$  for 1 M KCl,  $n = 1$ . Injected sample concentration in the eluent: 1 g/L. Other  
 295 experimental conditions: see Fig. 1.

296

297

298 **Table 1.** Hydrodynamic radius ( $R_h$ ) and molar mass ( $M_w$ ) determination by TDA using bare fused silica capillary (case 1) or PDADMAC/PSS SMIL-coated capillary (case 2) with  
 299 eluents of various ionic strengths. Eluent as indicated on the Table. Other TDA experimental conditions as in Fig. 1 or Fig. SI4 (case 1) or Fig. SI5 (case 2). RSD (%) or error bars  
 300 are calculated based  $\pm 1$  SD. Intra-capillary values based on  $n = 3$  determinations; inter-capillary values based on  $m = 3$  capillaries and  $n = 3$  repetitions per capillary. Eluant: 20 mM  
 301 Tris/HCl with 35.5 mM LiCl, pH 8. <sup>a</sup>Data given by the provider: anionicity by <sup>1</sup>H NMR,  $M_w$  and PDI by SEC-MALS for APAMs,  $M_w$  by SLS for IPAMs. <sup>b</sup>TDA molar masses were  
 302 obtained using the reciprocal of the least-squared regressions given in Fig. 2 (with  $M_w$  in  $10^6$  g/mol and  $R_h$  in nm)  $M_w = 0.00162 \times \langle R_h \rangle^{1.8706}$  (case 1) and  $M_w = 0.00195 \times \langle R_h \rangle^{1.7986}$   
 303 (case 2).

304  
305

	Anionicity (by <sup>1</sup> H NMR) <sup>a</sup>	$M_w$ (by SEC- MALS) <sup>a</sup> $\times 10^6$ g/mol)	PDI (by SEC-MALS) <sup>a</sup>	$M_w$ (by SLS) <sup>a</sup> $\times 10^6$ g/mol	Case 1 Bare-fused silica capillary			Case 2 SMIL-coated capillary		
					Intra-cap $\langle R_h \rangle_{\text{intra}}$ (nm)	Inter-cap $\langle R_h \rangle_{\text{inter}}$ (nm)	$M_{w, TDA}^b$ ( $10^6$ g/mol)	Intra-cap $\langle R_h \rangle_{\text{intra}}$ (nm)	Inter-cap $\langle R_h \rangle_{\text{inter}}$ (nm)	$M_{w, TDA}^b$ ( $10^6$ g/mol)
APAM1	26%	0.22±0.02	1.1±0.1		14.0 (3.0%)	13.4 (3.7%)		13.4 (3.0%)	13.5 (3.7%)	
APAM5	25%	0.80±0.1	1.2±0.2		30.0 (3.3%)	28.4 (7.0%)		28.0 (3.1%)	29.0 (3.2%)	
APAM10	29%	1.92±0.3	2.5±0.1		45.0 (4.0%)	43.0 (7.7%)		48.7 (5.4%)	47.0 (6.8%)	
APAM30	25%	3.93±0.5	1.4±0.2		55.0 (8.0%)	61.8 (8.9%)		68.7 (11%)	64.0 (7.8%)	
APAM50	30%	4.18±0.4	3.0±0.2		70.2 (12%)	80.6 (9.7%)		78.0 (7.3%)	80.0 (8.8%)	
APAM60	26%	7.34±0.7	1.5±0.2		104.0 (11%)	92.6 (8.9%)		103.0 (5.5%)	92.0 (8.5%)	
IPAM1	27%	4.3±0.4		6.5±0.7	70.0 (8.0%)	70.5 (3.5%)	4.3±0.4	75.5 (6.6%)	74.5 (4.8%)	4.7±0.2
IPAM2	28%			8±0.8	100.1 (9.1%)	91.2 (7.9%)	8.4±0.6	96.3 (2.4%)	93.7 (5.9%)	7.2±0.4
IPAM3	29%			10.5±1.1	114.2 (7.0%)	109.2 (8.7%)	12.3±1.1	106.6 (3.0%)	110.5 (6.8%)	9.7±0.7
IPAM4	33%			15±1.5	127.9 (8.1%)	131.9 (9.9%)	14.1±1.4	136.8 (2.9%)	138.4 (7.2%)	15.0±1.1
IPAM5	27%			25±2.5	167.0 (9.7%)	159.0 (9.5%)	20.8±2.0	191.3 (6.0%)	183.7 (7.0%)	25.2±1.8

306

### 307 **3.2. Impact of BGE ionic strength using fused silica capillary**

308 To possibly extend the range of molar masses that can be analyzed by TDA; higher eluent  
309 ionic strengths were used to get more compact polyelectrolyte conformations by screening of  
310 the electrostatic repulsions between charged monomers in the polyelectrolyte chain.  
311 Accordingly, the BGE (20 mM Tris/HCl) was completed by adding 1 M NaCl or 1 M KCl  
312 (instead of 35.5 mM LiCl) in order to investigate the impact of high ionic strength on the  $R_h$   
313 determined by TDA for APAM and IPAM samples. Open symbols in Fig. 2 shows the  $\log R_h$   
314 –  $\log M_w$  correlations obtained at 1 M NaCl and 1 M KCl on bare fused silica capillaries. As  
315 expected lower  $R_h$  values were obtained at 1 M NaCl (or KCl) with a decrease by a factor  $\sim$   
316 1.5 compared to 35.5 mM LiCl, while the correlation was slightly lower at high ionic strength  
317 ( $R^2 = 0.9926$  at 35.5 mM LiCl compared to  $R^2 = 0.9613$  at 1M NaCl, and  $R^2 = 0.9686$  at 1 M  
318 KCl). The expected decrease in hydrodynamic radii of the polymers at high ionic strengths  
319 was similar in 1 M KCl and in 1 M NaCl.

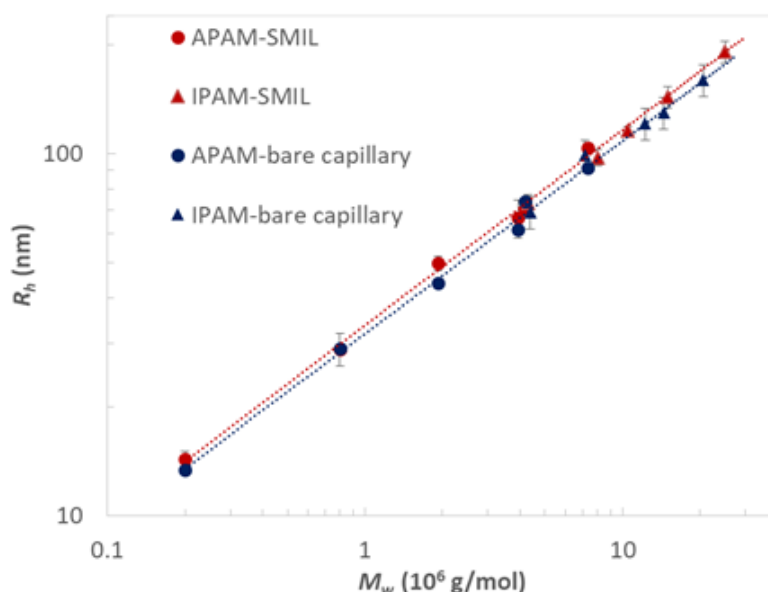
320

### 321 **3.3. SMIL-coated capillary**

322 Fig. 3 compares the  $\log R_h$  –  $\log M_w$  correlations achieved with APAMs and IPAMs using a  
323 bare-fused silica capillary and a SMIL coated capillary (20 mM Tris/HCl with 35.5 mM LiCl  
324 eluant). Two PADMAC/PSS bilayers were deposited on the silica capillary by simple flushes  
325 (see section 2.5 for experimental protocol), to enhance electrostatic repulsion between the  
326 capillary wall and the polyelectrolyte analytes. The purpose of this SMIL coating was to  
327 decrease the consuming rinsing time between runs (30 min on fused silica capillary vs 8 min  
328 on SMIL coated capillary), and possibly to get better reproducibility in the taylorgrams, and  
329 consequently lower RSD in the  $R_h$  determination. The correlation lines were very close to  
330 each other on the two type of capillaries with similar scaling laws and correlation coefficients:  
331  $\langle R_h \rangle = 32.145 \times M_w^{0.5560}$ ,  $R^2 = 0.9910$  (SMIL-coating) and  $\langle R_h \rangle = 31.020 \times M_w^{0.5346}$ ,  $R^2 =$   
332  $0.9926$  (bare fused silica capillary), with  $M_w$  in  $10^6$  g/mol and  $R_h$  in nm. The molar masses of  
333 IPAMs were then derived from  $\langle R_h \rangle$  using the reciprocal of the scaling laws and reported in  
334 Table 1. The TDA results with RSD in the range of 3-12% are in good agreement with the  
335 SLS-ones ( $\sim 10\%$  discrepancies). Comparing the two protocols, SMIL-coating method is  
336 advantageous over fused silica capillary for time-saving (8 min rinsing time between runs  
337 instead of 30 min) and more symmetric taylorgrams (see Fig. SI4/SI6 and Fig. SI5/SI7).  
338 SMIL coating also provided better intra and inter capillary RSD for the polydisperse IPAM  
339 samples. It is worth noting that the stability of SMIL coated capillaries sustained throughout  
340 the repeatability assay of all the samples. Compared to the upper limit in molar mass obtained

341 in CGE ( $M_w < 10$  MDa [13]), TDA extended the accessible molar mass range up to 25 MDa  
342 for IPAM copolymers.

343



344

345 **Figure 3.**  $\log R_h - \log M_w$  plots for poly(acrylic acid-co-acrylamide)s standards (APAMs) and industrial samples  
346 (IPAMs) obtained using a bare fused silica capillary (blue) or a SMIL-coated capillary (red). Experimental  
347 conditions: capillary dimensions, 50  $\mu\text{m}$  ID  $\times$  60 cm (50 cm to the detector). Eluent: 20 mM Tris/HCl with 35.5  
348 mM LiCl,  $I = 46.5$  mM, pH 8.0. Mobilization pressure: 0.4 psi. Injection: 0.5 psi, 7 s. Injected sample  
349 concentration: 2 g/L in eluent. SMIL consisted of two bilayers of PDADMAC/PSS at a polymer concentration of  
350 3 g/L (see experimental part for more details). Rinsing between runs: fused silica capillary, 1 M NaOH at 35 psi  
351 for 10 min, 0.1 M NaOH at 20 psi for 5 min, Milli-Q water at 20 psi for 5 min and BGE at 20 psi for 10 min.  
352 SMIL coated capillary: BGE at 20 psi for 8 min. UV detection at 200 nm. Temperature: 25°C. The calibration  
353 lines established with APAMs read with  $M_w$  in  $10^6$  g/mol and  $R_h$  in nm:  $\langle R_h \rangle = 32.145 \times M_w^{0.5560}$ ,  $R^2 = 0.9910$   
354 (SMIL coated capillary);  $\langle R_h \rangle = 31.020 \times M_w^{0.5346}$ ,  $R^2 = 0.9926$  (bare fused silica capillary). Error bars are  $\pm$  one  
355 SD. Other experimental conditions: see Fig. 1.

356

#### 357 4. Conclusion

358 TDA was proven straightforward and powerful for size determination of a wide range of  
359 anionic polyacrylamides of hydrodynamic radii from 10 to 190 nm. The molar mass of the  
360 industrial samples were deduced from these hydrodynamic radii and found between 4.3 MDa  
361 and 25 MDa. The data processing of the taylorgrams comprised Gaussian fitting with  
362 subtraction of the contribution from small impurities, determination of hydrodynamic radii of  
363 the polymers, calibration using  $\log R_h - \log M_w$  correlation with standards characterized by  
364 SEC-MALS, and thereafter calculation of molar masses of industrial samples. Two protocols  
365 were employed and compared, aiming at improving  $R_h - M_w$  correlation and repeatability /  
366 reproducibility. A first protocol was based on bare fused silica capillaries and intensive

367 between-run rinsing (30 min), the other was based on SMIL-coated capillaries and simple  
368 rinsing (8 min). Both cases led to consistent results that are in agreement with those  
369 determined by SLS within relative error deviation. So far, TDA provided a new, reliable  
370 methodology of sized-based molar mass determination far beyond the detection limits of SEC  
371 (< 7.3 MDa) and also a convenient alternative to SLS. Last but not least, the concern of high  
372 polymer aggregation under action of electric fields encountered in CGE was fully alleviated  
373 in TDA due to orthogonal techniques based on completely different principles. As a  
374 perspective, it would be interesting to investigate the polyelectrolyte polydispersity by TDA  
375 using constraint regularized linear inversion approach for the fitting of the taylorgrams. To  
376 that respect, improving the signal to noise ratio could be of interest.

377

## 378 **References**

- 379 [1] A. Thomas, N. Gaillard, C. Favero, Some key features to consider when studying  
380 acrylamide-based polymers for chemical Enhanced Oil Recovery, *Oil Gas Sci.*  
381 *Technol.* 67(6) (2013) 887-902, doi: 10.2516/ogst/2012065.
- 382 [2] A.G. Guezennec, C. Michel, K. Bru, S. Touze, N. Desroche, I. Mnif, M. Motelica-  
383 Heino, Transfer and degradation of polyacrylamide-based flocculants in hydrosystems:  
384 a review, *Environ. Sci. Pollut. Res. Int.* 22 (2015) 6390–6406, doi: 10.1007/s11356-  
385 014-3556-6.
- 386 [3] A. Sabhapondit, A. Borthakur, I. Haque, Characterization of acrylamide polymers for  
387 enhanced oil recovery, *J. Appl. Polym. Sci.* 87 (2003) 1869–1878, doi :  
388 10.1002/app.11491.
- 389 [4] L. Rodriquez. Thesis : Analyse dimensionnelle, comportement thermique et  
390 mécanique de polymères en solution aqueuse à base de 2-acrylamido-2-méthylpropane  
391 sulfonate : Application en Récupération Assistée d'Hydrocarbures. Université de Pau  
392 et des Pays de l'Adour (2016).
- 393 [5] A. Müller, L. Patruyo, W. Montano, D. Roversi-M, R. Moreno, N. Ramírez, A. Sáez,  
394 Mechanical degradation of polymers in flows through porous media: effect of flow  
395 path length and particle size, *Appl. Mech. Rev.* 50 (1997) 149-155, doi:  
396 10.1115/1.3101827
- 397 [6] T.Q. Nguyen, H.H. Kausch, Chain scission in transient extensional flow kinetics and  
398 molecular weight dependence, *J. Non-Newton. Fluid. Mech.* 30 (1988) 125–140, doi:  
399 10.1016/0377-0257(88)85020-1.
- 400 [7] S. Jouenne, M. Loriau, B. Grassl, N. Andreu, Method for determining the weight-  
401 average molecular weight of a water-soluble high molecular weight polymer, Patent  
402 WO 2017042603 A1 2017031 (2017).
- 403 [9] J. Wang, H. Huang, X. Huang, Molecular weight and the Mark-Houwink relation for  
404 ultra-high molecular weight charged polyacrylamide determined using automatic batch  
405 mode multi-angle light scattering, *J. Appl. Polym. Sci.* 133 (2016) 43748, doi:  
406 10.1002/app.43748.
- 407 [10] B.A. Buchholz, A.E. Barron, The use of light scattering for precise characterization of  
408 polymers for DNA sequencing by capillary electrophoresis, *Electrophoresis* 22 (2001)

- 409 4118–4128, doi: 10.1002/1522-2683(200111)22:19<4118::AID-ELPS4118>3.0.CO;2-  
410 Q.
- 411 [11] Y. Dalsania, A. Doda, J. Trivedi, Characterization of ultrahigh-molecular-weight  
412 oilfield polyacrylamides under different pH environments by use of asymmetrical-flow  
413 field-flow fractionation and multiangle-light-scattering detector, *SPE J.* 23 (2018) 48-  
414 65, doi: 10.2118/174624-PA.
- 415 [12] M. Leeman, M. T. Islam, W. G. Haseltine, Asymmetrical flow field-flow fractionation  
416 coupled with multi-angle light scattering and refractive index detections for  
417 characterization of ultra-high molar mass poly(acrylamide) flocculants, *J.*  
418 *Chromatogr. A* 1172 (2007) 194-203, doi: 10.1016/j.chroma.2007.10.006.
- 419 [13] X. Leclercq, L. Leclercq, A. Guillard, L. Rodriguez, O. Braun, C. Favero, H. Cottet,  
420 Characterization of ultrahigh molar mass polyelectrolytes by capillary electrophoresis,  
421 *J. Chromatogr. A* 1631 (2020) 461536, doi: 461536,  
422 ff10.1016/j.chroma.2020.461536ff.
- 423 [14] S. Magnúsdóttir, H. Isambert, C. Heller, J.L. Viovy, Electrohydrodynamically induced  
424 aggregation during constant and pulsed field capillary electrophoresis of DNA,  
425 *Biopolymer* 49 (1999) 385–401, doi: 10.1002/(SICI)1097-0282(19990415)49:5<385::  
426 AID-BIP5>3.0.CO;2-L.
- 427 [15] L. Leclercq, S. Reinhard, J. Chamieh, M. Döblinger, E. Wagner, H. Cottet, Fast  
428 characterization of polyplexes by Taylor dispersion analysis, *Macromolecules* 48  
429 (2015) 7216–7221, doi: 10.1021/acs.macromol.5b01824.
- 430 [16] H. Cottet, M. Martin, A. Papillaud, E. Souaid, H. Collet, A. Commeyras,  
431 Determination of dendrigraft poly-L-Lysine diffusion coefficients by Taylor dispersion  
432 analysis. *Biomacromolecules* 8 (2007) 3235-3243, doi: 10.1021/bm070268j.
- 433 [17] H. Cottet, J.-P. Biron, L. Cipelletti, R. Matmour, M. Martin, Determination of  
434 individual diffusion coefficients in evolutive binary mixtures by Taylor dispersion  
435 analysis: application to the monitoring of polymer reaction, *Anal. Chem.* 82 (2010)  
436 1793-1802, doi: 10.1021/ac902397x.
- 437 [18] J. P. Biron, F. Bonfils, L. Cipelletti, H. Cottet, Size-characterization of natural and  
438 synthetic polyisoprenes by Taylor dispersion analysis, *Polymer Testing* 66 (2018) 244-  
439 250, doi: 10.1016/j.polymertesting.2018.01.017.
- 440 [19] F. d'Orlye, A. Varenne, P. Gareil, Determination of nanoparticle diffusion coefficients  
441 by Taylor dispersion analysis using a capillary electrophoresis instrument, *J.*  
442 *Chromatogr. A* 1204 (2008) 226–232, doi: 10.1016/j.chroma.2008.08.008.
- 443 [20] D. A. Urban, A. M. Milosevic, D. Bossert, F. Crippa, T. L. Moore, C. Geers, S. Balog,  
444 B. Rothen-Rutishauser, A. Fink, Taylor Dispersion of inorganic nanoparticles and  
445 comparison to dynamic light scattering and transmission electron microscopy, *Colloid*  
446 *Interface Sci. Commun.* 22 (2018) 29–33, doi:10.1016/j.colcom.2017.12.001.
- 447 [21] L. Cipelletti, J.-P. Biron, M. Martin, H. Cottet, Measuring arbitrary diffusion  
448 coefficient distributions of nano-objects by Taylor dispersion analysis, *Anal. Chem.* 87  
449 (2015) 8489–8496, doi: 10.1021/acs.analchem.5b02053.
- 450 [22] J. Chamieh, L. Leclercq, M. Martin, S. Slaoui, H. Jensen, J. Østergaard, H. Cottet,  
451 Limits in size of Taylor dispersion analysis: Representation of the different  
452 hydrodynamic regimes and application to the size-characterization of cubosomes.  
453 *Anal. Chem.* 89 (2017) 13487–13493, doi: 10.1021/acs.analchem.7b03806.
- 454 [23] A. Hawe, W.L. Hulse, W. Jiskoot, R.T. Forbes, Taylor dispersion analysis compared  
455 to dynamic light scattering for the size analysis of therapeutic peptides and proteins  
456 and their aggregates, *Pharm. Res.* 28 (2011) 2302–2310, doi: 10.1007/s11095-011-  
457 0460-3.



- 458 [24] C. Malburet, L. Leclercq, J-F Cotte, J. Thiebaud, S. Marco, M.-C. Nicolai, H. Cottet,  
459 Antigen-adjuvant interactions in vaccines by Taylor dispersion analysis: Size  
460 characterization and binding parameters, *Anal. Chem.* 93 (2021) 6508–6515, doi:  
461 10.1021/acs.analchem.1c00420.
- 462 [25] H. Cottet, J.-P. Birona, M. Martin, On the optimization of operating conditions for  
463 Taylor dispersion analysis of mixtures, *Analyst* 139 (201) 3552-3562, doi:  
464 10.1039/c4an00192c.
- 465 [26] E. Read, A. Guinaudeau, D.J. Wilson, A. Cadix, F. Violleau, M. Destarac, Low  
466 temperature RAFT/MADIX gel polymerization: access to controlled ultra-high molar  
467 mass polyacrylamides, *Polym. Chem.* 5 (2014) 2202– 2207, doi: 10.1039/c3py01750h.
- 468 [27] G. Taylor, Dispersion of soluble matter in solvent flowing slowly through a tube, *Proc.*  
469 *R. Soc. London, Ser. A* 219 (1953) 186-203, doi: 10.1098/rspa.1953.0139.
- 470 [28] R. Aris, On the dispersion of a solute in a fluid flowing through a tube, *Proc. R. Soc.*  
471 *London, Ser. A* 235 (1956) 67-77, doi: 10.1098/rspa.1956.0065.
- 472 [29] M. S. Bello, R. Rezzonico, P. G. Righetti, Use of Taylor-Aris dispersion for  
473 measurement of a solute diffusion coefficient in thin capillaries, *Science* 266 (1994)  
474 773-776, doi: 10.1126/science.266.5186.773.
- 475 [30] G. S. Manning, Limiting Laws and counterion condensation in polyelectrolyte  
476 solutions I. Colligative properties, *J. Chem. Phys.* 51 (1969) 924, doi:  
477 10.1063/1.1672157.
- 478 [31] J.Lecourtier, L.T. Lee, G. Cheveteau, Adsorption of polyacrylamides on siliceous  
479 minerals, *Colloids & Surfaces*, 47 (1990) 219-231, doi: 10.1016/0166-  
480 6622(90)80074-E.
- 481 [32] H. Bessaies-Bey, J. Fusier, S. Harrisson, M. Destarac, S. Jouenne, N. Passade-Boupat,  
482 F. Lequeux, J.-B. d'Espinose de Lacaillerie, N. Sanson, Impact of polyacrylamide  
483 adsorption on flow through porous siliceous materials: State of the art, discussion and  
484 industrial concern, *J. Colloid Interface Sci.* 531 (2018) 693-704, doi:  
485 10.1016/j.jcis.2018.07.103.
- 486 [33] A. Samanta, A. Bera, K. Ojha, A. Manda, Effects of alkali, salts, and surfactant on  
487 rheological behavior of partially hydrolyzed polyacrylamide solutions, *J. Chem. Eng.*  
488 *Data* 55 (2010) 4315–4322, doi: 10.1021/je100458a.
- 489 [34] L. Leclercq, M. Morvan, J. Koch, C. Neusuess, H. Cottet, Modulation of the  
490 electroosmotic mobility using polyelectrolyte multilayer coatings for protein analysis  
491 by capillary electrophoresis, *Anal. Chim. Acta* 1057 (2019) 152-161, doi:  
492 10.1016/j.aca.2019.01.008.
- 493 [35] S. Bekri, L. Leclercq, H. Cottet, Polyelectrolyte multilayer coatings for the separation  
494 of proteins by capillary electrophoresis: influence of polyelectrolyte nature and  
495 multilayer crosslinking, *J. Chromatogr. A* 1399 (2015) 80-87, doi:  
496 10.1016/j.chroma.2015.04.033.
- 497